IOSR Journal of Mechanical and Civil Engineering (IOSR-JMCE)
e-ISSN: 2278-1684,p-ISSN: 2320-334X, Volume 14, Issue 5 Ver. IV (Sep. - Oct. 2017), PP 01-08
www.iosrjournals.org

Effect of Rotor Position on Wind Loads Acting on the Tower of a Stopped Wind Turbine

Anabel Apcarian[1] and Jorge Lässig[2]
[1,2](Faculty of Engineering, Universidad Nacional del Comahue, Neuquén, Argentina)

Abstract: *The north part of the Neuquén province in Argentina is a region of great wind potential, where high-powered wind turbine parks are currently being under construction. Due to the local wind conditions, the supporting structure of the aerogenerators has to face extreme conditions far from what regulations recommend. A special load case appears when, during a windstorm, the rotor remains stationary in a feathered pitch position. Control mechanisms stop the rotor to protect the turbine integrity, but it is impossible to determine in which position this will happen. This paper aims to study the effect of the rotor position over the wind loads that act on a multi-MW wind turbine tower subjected to extreme typical winds in the Auquinco region in Neuquén. A 1:75 scale aerogenerator tower model was tested in a boundary layer wind tunnel with the aerogenerator stationary in a feathered pitch attitude for two rotor positions. Results suggest that the most favorable position is the one with no blades in front of the tower.*
Keywords: *wind turbine tower, wind loads, extreme winds, wind tunnel tests.*

Date of Submission: 27-09-2017 Date of acceptance: 18-10-2017

I. Introduction

The wind power industry in Argentina has shown a fast growth in the last years thanks to the support of various national programs that promote the use of reusable energy sources aimed to the production of electric energy. To quantify the wind resource availability, a series of projection plans was designed. Among the results of these studies is the one of the Neuquén province, in which the feasibility study of an eolic park performed by the Provincial Office of Energy Sources (Ente Provincial de Energía del Neuquén, 2010 [1]), determined that in the north of the province, specifically in the Auquinco region, there are adequate winds for the generation of electric energy (Figure 1). Based on the obtained results, eolic parks with 2 to 3 MW power aerogenerators were designed. The turbines will feature tapered tubular steel towers of 80 m mean high. Due to the local wind conditions, these structures will have to face extreme conditions that are far from what design regulations recommend.

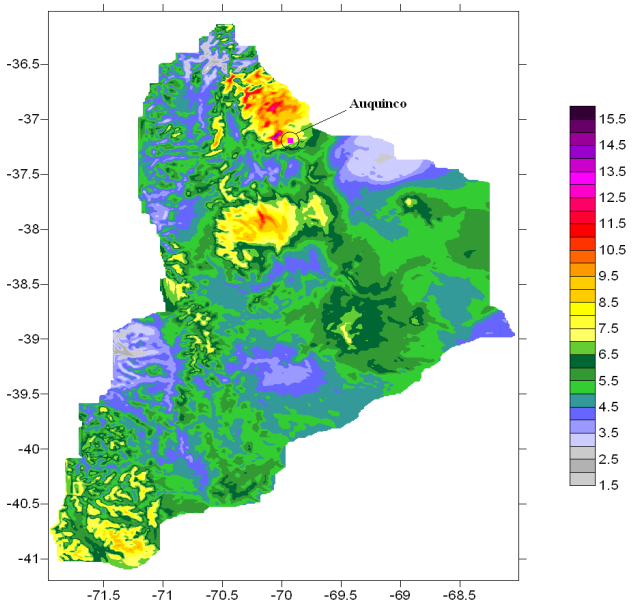

Figure 1: Wind velocity distribution in m/s at 70 m high over Neuquén (Lat. 37° 19' 06", Long. 69° 56' 53", a.o.s.l. 1554 m)

Specific studies performed in the region Palese and Lässig (2006 [2]); Lässig, Palese, Cogliati et. al. (1999 [3]) describe the wind of the region as intense and very turbulent, with gusts that occur every 3 minutes and that exceed an angle of 20° in the change of the wind course. For this type of wind, the IEC 61400-1(2005 [4]) standard establishes that the meteorological parameters required for design have to be defined by the manufacturer. The EWTS II (1999 [5]) standard coincides and recommends a wind validation *in-situ.*

Storms and extreme wind conditions are a critical charge state to which turbine control mechanisms stop the rotor to avoid mechanical or structural failures due to fatigue processes. In high power generators, the breaking procedure includes a blade rotation until the trailing edge is aligned with the wind direction, reached by the position named *feathered pitch*. Once the rotor is stationary, the blades are randomly positioned in front of the tower, which is being subjected to wind loads of great magnitude.

The main purpose of this work was to study the effect of the rotor position in the acting wind loads over the tower of a multi-MW aerogenerator subjected to extreme winds in the Auquinco region.

II. Methodology

II.1.- Wind data applied for the region under study

The wind data of the Auquinco region applied for this study was obtained from a meteorological station installed in Auquinco during 2007 and 2009. The measuring system is comprised of an NRG System datalogger brand Symphonie, two NRG#40 speed sensors located at 10 and 30 m high, an NRG#200P orientation sensor located at 30 m; and an NRG 110S temperature sensor located 3m away. All the sensors are calibrated and they register the main values, minimum, maximum, and std. deviation of each sensor in 10-minute intervals. The sensors present a good performance in the presence of predominant winds. The calculation of the extreme winds can be found at Lässig, Palese and Apcarian (2011 [6]).

For a reference height z_R= 30 m, the following data was obtained: extreme wind velocity with return period of 50 yrs = 79 m/s; mean velocity = 8 m/s; power law coefficient = 0.05; mean turbulence intensity = 18.2 %; turbulence intensity with extreme winds = 9%-10%.

II.2._ Wind tunnel used for this study

The tests performed for this study were carried out in the open circuit boundary layer wind tunnel installed in the Laboratory of Boundary Layer and Environmental Fluid Dynamics of the Faculty of Engineering of the University of La Plata. The tunnel is 24 m long with a cross-sectional constant of 2.60 m x 1.80 m. It works by means of aspiration and features nine fans, each one being 1.25 m long in diameter and with a power of 15HP. The maximum test velocity is 15 m/s.

II.3.- Prototype selection and model construction

A representative aerogenerator similar to the ones that will be installed in the region was used as a prototype (Figure 2). It features an horizontal axis, three blades, it is orientated windward, and has a tapered steel tower. The model was built in wood, on a 1:75 scale (Figure 3).

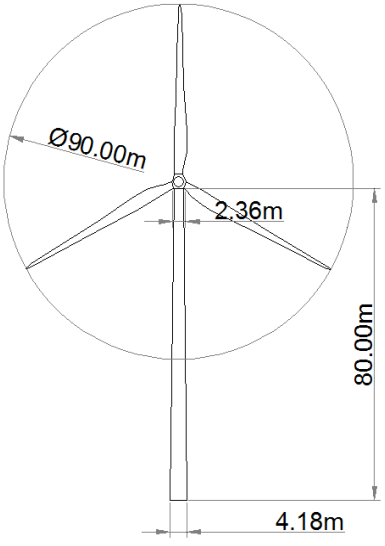

Figure 2: Prototype dimensions.

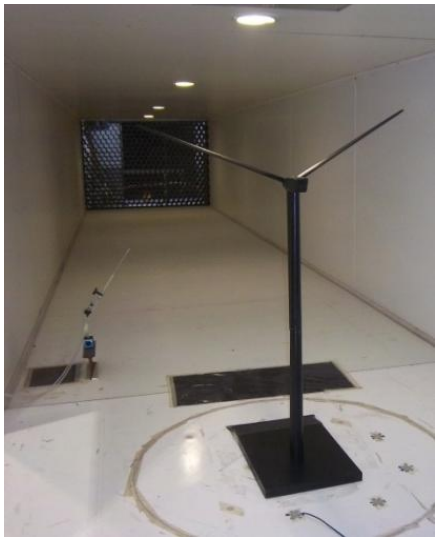

Figure 3: Model installed in the wind tunnel.

II.4.- Rotor positions

Tests were conducted for the two positions of the rotor that are indicated in Figure 4, as any other position would be positioned between these two.

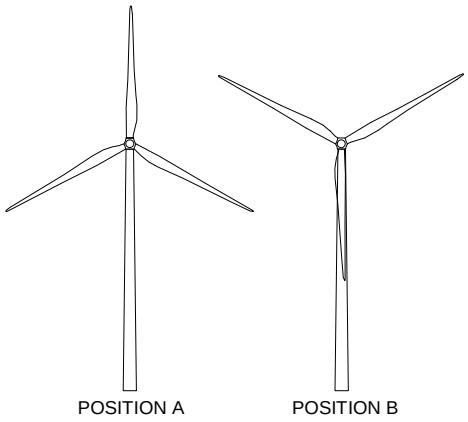

Figure 4: Rotor positions used during the tests.

II.5.- Dimensional similitude analysis

Reynolds number conservation

As it is not possible to maintain Reynolds number (Re) because the prototype's **Re** was greater than the one of the model´s in several orders of magnitude, a mock-up with the maximum scale permitted by the test section was built (1:75). Tests were performed with the maximum possible velocity (15 m/s) provided by the tunnel. Under these conditions, it was verified that the separation points in the mock-up would coincide with the prototype´s and that the flow would be the same. The maximum Re reached was 4.37×10^4.

Incompressible flow conservation

Using the extreme velocity of a 50-year return using the *k* parameter of the 10-minute mean winds Weibull distribution in the prototype, a Mach number (**Ma**) of $\mathbf{Ma}_{prototype}$ =0.24 is obtained. Furthermore, if the extreme map form velocity suggested by the CIRSOC 102 (2005 [7]) regulations is applied, then a $\mathbf{Ma}_{prototype}$ =0.13 is obtained. In the model, considering the maximum flow upstream velocity then $\mathbf{Ma}_{model}$= 0.04. These values indicate that the flow remains incompressible.

Jensen number conservation

Roughness level for the prototype (z_{0p}) lies between 0.01 m and 0.001 m. Adopting the mean value z_{0p} = 0.0055 m, the prototype Jensen number (**Je**) is $\mathbf{Je}_{prototype}$= 80/0,0055 = 14,545.45. In the model a z_{0m} = 0.00007 m was applied, obtaining a $\mathbf{Je}_{model}$= 1.07/0.00007 = 15,285.7. Both **Je** values are of the same order and greater than 2000, which is a value from which the pressure coefficient is no longer a function of the Jensen number, as explained by Dyrbye and Hansen (1997[8]). Therefore, this condition of similarity applies.

Characterization of the wind in the tunnel

At test velocity, the velocity profile of the boundary layer in the model is similar to the one of the prototype´s. Thus, an almost uniform profile is obtained (Figure 5). The power law coefficient (α in the model was 0.02, while the prototype featured a coefficient of α =0.05.

The intensity of turbulence (*TI*) in the region of study during a windstorm (wind velocity $V \geq 30$ m/s) is less than 10% and in the wind tunnel values smaller than 5% were achieved. By implementing elements that would increase roughness, the turbulence inside the wind tunnel was then increased. However, these factors greatly influenced the boundary layer profile and therefore, it was decided to maintain the profile similarity of the model and the prototype at expenses of a minor turbulence intensity in the model.

Due to the tower geometry, the fluid dynamic characteristics of the problem are greatly affected by the Reynolds number. However, according to Flay (2013 [9]), maintaining the Jensen number of the model and the prototype, it is possible to obtain a distribution of pressure very similar to the real scenario. Moreover, according to Crowe, Elger and Roberson (2002 [10]), the pressure coefficient (*Cp)* stabilizes for Reynolds numbers greater than 100,000.

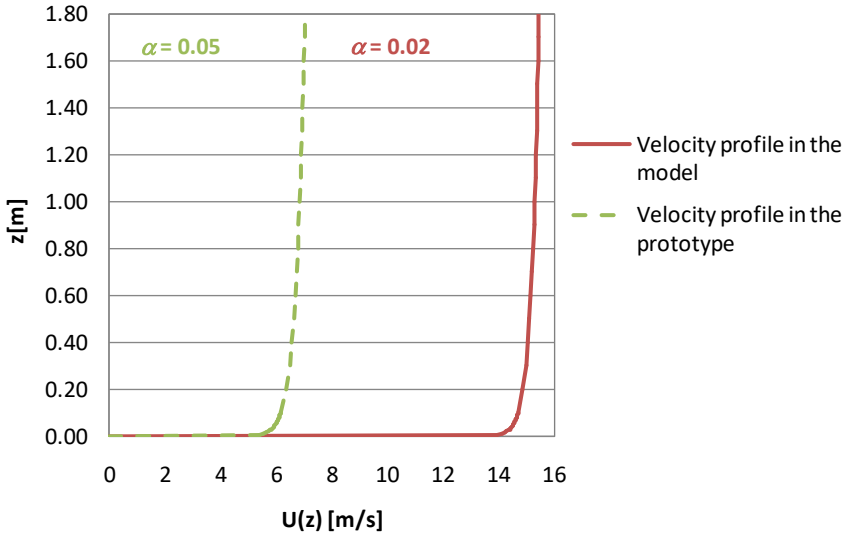

Figure 5: Velocity profiles in the prototype and in the model showing the variation of the incoming wind velocity (U) as a function of the height from the ground (z).

II.6.- Pressure measurements test

The main purpose of this test was to calculate the *Cp* coefficient in several points of the tower and analyze its variation according to the rotor position. Eight pressure-measuring points were placed half way to the top of the tower as indicated in Figure 6. The static pressure-measuring points were connected to a micromanometer ALNOR EBT 721 and measurements were taken for both rotor positions A and B. The wind velocity in the tunnel was measured with a micromanometer TESTO 512

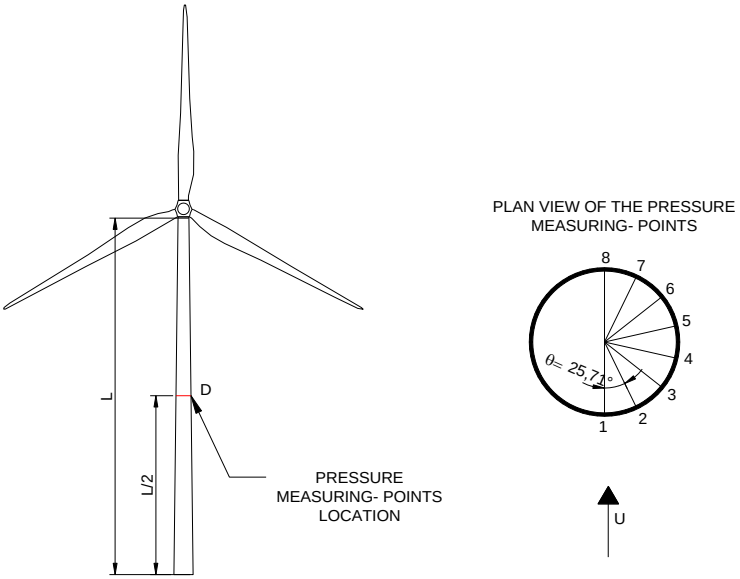

Fig. 6: Pressure-measuring points location

II.7.- Test to determine the dynamic characteristics of the flow in the wake

The main objective of this test was to study the velocity variations and turbulence intensity *(TI)* in the wake of the tower that are created when the rotor position is modified. The instant velocity of the flow was therefore, measured in three points behind the tower, indicated in Figure 7. The measuring plan distance to the tower was of one diameter.

Data was collected by means of a two-pins hot-wire anemometer DANTEC STREAMLINE at a constant temperature. Data collection frequency was 2000 Hz and a low-pass filter of 1000 Hz was also applied. Only the horizontal component of the flow was analyzed, as it was the most significant one, given the fact that the velocity values in the cross-sectional direction were too small.

With the obtained data, the mean velocity u_m and the *TI* were calculated on each point

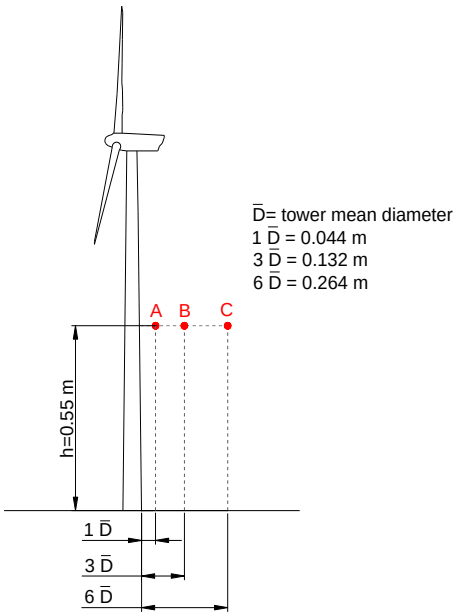

Figure 7: Wake points where the wind velocity was measured.

III. Results

The pressure values obtained during this study are indicated in table 1. The graphics indicate these values as a function of the angular position θ in the measurement of Figure 8 for rotor positions A and B.

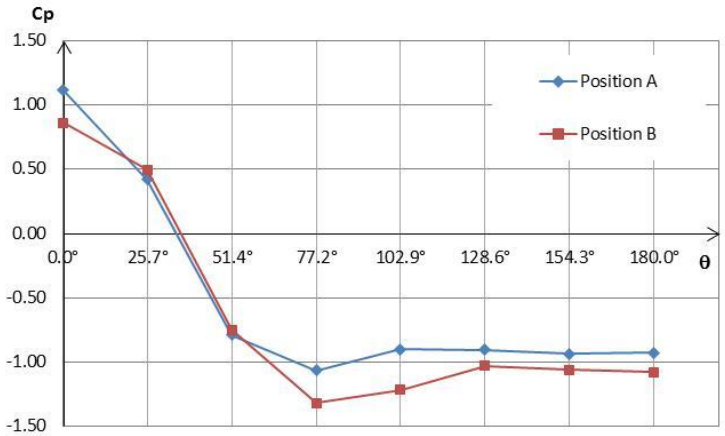

Fig. 8: *C_p distribution in the cross-sectional area*

Table 2: C_p coefficient obtained values

Point N°	θ [°]	Position with blade		Position with no blade	
		Pressure [Pa]	C_p	Pressure[Pa]	C_p
1	0	154	1	119	0.74
2	25.71	57.8	0.29	68,2	0.37
3	51.43	-109	-0.91	-103	-0.87
4	77.14	-147	-1.19	-182	-1.44
5	102.9	-124	-1.02	-168	-1.34
6	128.6	-125	-1.03	-142	-1.15
7	154.3	-129	-1.06	-146	-1.18
8	180.0	-128	-1.05	-149	-1.20

Table 3 shows the wind velocity measurements obtained in the wake of the tower. Figures 9, 10 and 11 feature the power spectral density of the velocity component referred to the flow direction at 1D, 3D and 6D respectively.

***Table 3**: Obtained results of the wind measurements on the wake*

Rotor positions	Mean velocity [m/s]			Turbulence intensity [%]		
	1D	3D	6D	1D	3D	6D
A	19.38	15.94	16.10	7.14	16.30	10.53
B	18.76	16.36	16.46	5.37	12.50	7.94

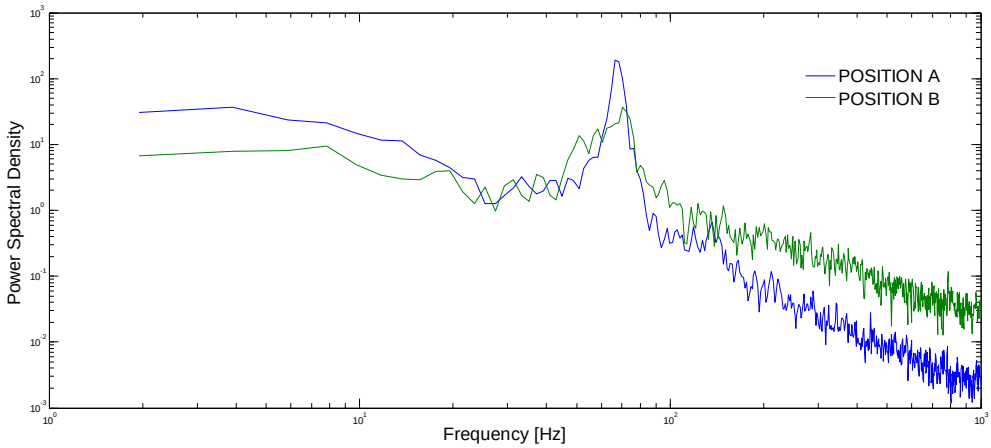

Figure 9: Power spectral density of the velocity component referred to the flow direction at 1D distance from de tower

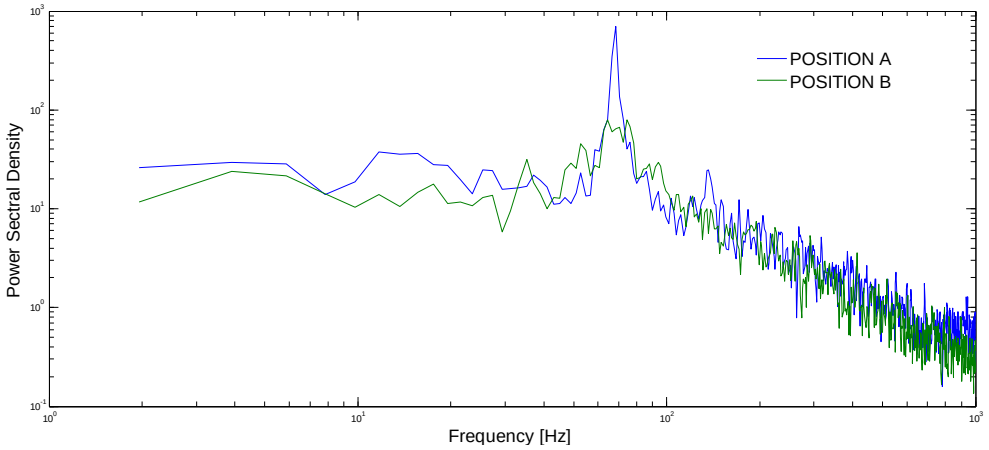

***Figure 10:** Power spectral density of the velocity component referred to the flow direction at 3D distance from de tower*

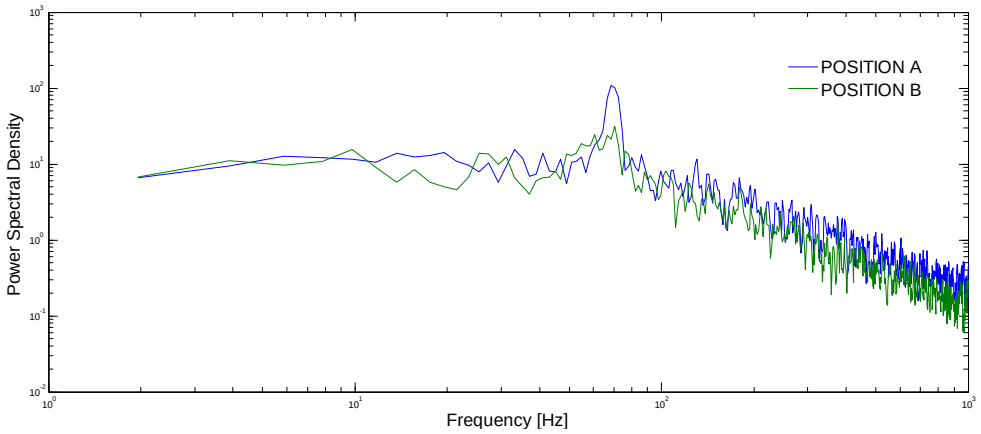

***Figure 11:** Power spectral density of the velocity component referred to the flow direction at 6D distance from de tower*

IV. Discussion

Figure 8 shows that with no blade in front of the tower the flow separation occurs before reaching a 120° angle, whereas when the blade is in front of the tower, the separation happens at an angle greater than 120°.

In both cases, the sign inversion of the pressure occurs between angles of 25.7° and 51.43°. The position of the rotor does not produce changes in the sign of the C_p coefficient. However, the variation in the pressure intensity modifies the windward area subjected to positive pressure, as it can be inferred in Figure12.

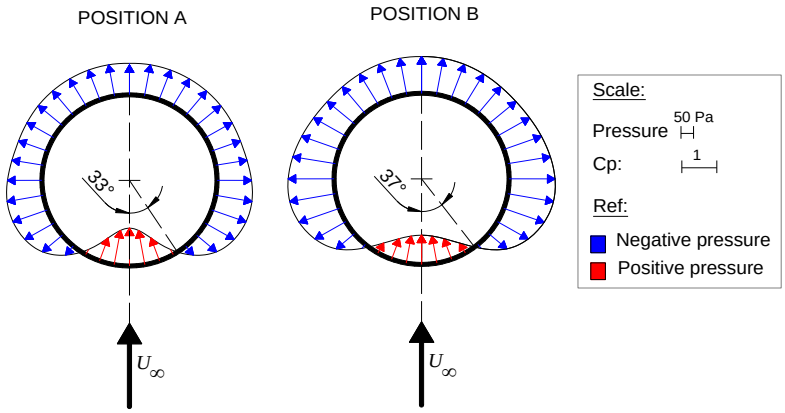

Figure 12: Graphic estimation of the distribution of pressures in the cross-sectional area.

Generally, the windward blade effect reduces the turbulence intensity and the wind velocity in the wake (except at a distance of 3 diameters where velocity increases).

The variation of the power spectral density with the rotor position indicated that the top frequency, with the windward blade, is shifted 6 Hz approximately compared with the tower with no blade (From 66.41 Hz to 72.27 Hz at 1 diameter; from 68.13 Hz to 74.23 Hz at 3 diameters). At six diameters of distance, the power spectral density shifted only 2 Hz (from 68.37 Hz to 70.32 Hz).

In addition, it is possible to observe that holding the blade windward to the tower, the maximum frequency is not a peak but a bandwidth of approximately 10 Hz.

V. Conclusion

The rotor position modifies the pressure distribution in the tower perimeter. The variation percentage at each point of the cross-sectional area is a function of its relative position to the incidental flow.

It is inferred that, though it reduces the positive stagnation pressure, the presence of a blade in front of the tower increases the wake suction, which results in the growth of the horizontal pressure force over the regions of the tower under study.

Moreover, the presence of the blade against the tower produces greater tower lateral velocities, causing greater lateral suction and thus creating additional lateral loads (crosswise) on the tower.

The variations of the rotor position create changes in the wind velocity and its turbulence intensity on the tower wake.

In general, the presence of the blade in front of the tower increases the bandwidth in the case of the main frequencies of vortex shedding. It also increases the drag force in 10.84% and lateral suction in 29%.

The best rotor position from a structural standpoint is with no blade in front of the tower.

Acknowledgements

This work is made from founded research projects of the National University of Comahue. The authors thank the director of the Laboratory of Environmental Fluid Dynamics Boundary Layer and the National University of La Plata, Dr. Julio Maranon Di Leo and his research group formed by Dr. Sebastian Delnero, Ing. Victor Manuel Padilla and Mr. Nehuén Savloff, who made possible to carry out the tests.

References

[1]. Ente Provincial de Energía del Neuquén. (2010). Prefactibilidad Técnica y Prediseño de Parque Eólico en Auquinco, Neuquén. Neuquén.

[2]. Palese, C., & Lässig, J. (2006). Mapa eólico de la provincia del Neuquén. Hidrored Red Latinoamericana de Micro Hidroenergía, II(ISSN: 0935-0578), pps. 03-11.

[3]. Lässig, J., Palese, C., Cogliati , M., & Bastanski, M. (1999). Wind characteristics in Neuquén, North Patagonia, Argentina. Journal of Wind Engineering and Industrial Aerodynamics, 79, pps. 183-199.

[4]. International Electrotechnical Comission. (2005). International Standard IEC 61400-1: Wind turbine generator systems. Part 1: Safety requirements. Geneve: IEC.
[5]. Pierik, J., Dekker, J., Braam, H., Bulder, B., Winkelaar, D., Larsen, G., et all. (1999). European wind turbine standards II (EWTS-II). En E.
[6]. Lässig, J. L., Palese, C., & Apcarian, A. (2011). Vientos extremos en la provincia de Neuquén. (C. A. Meteorólogos, Ed.) Meteorológica, 36(2), pps. 83-93.
[7]. CIRSOC 102: Centro de Investigación de los Reglamentos Nacionales de Seguridad para las Obras Civiles del Sistema INTI. (2005). Reglamento Argentino de Acción del Viento sobre las Construcciones. Buenos Aires: INTI Instituto Nacional de Tecnologia Industrial.
[8]. Dyrbye, C., & Hansen, S. (1997). Wind loads on structures. E, New York: John Wiley & Sons Publishers.
[9]. Flay, R. (2013). Bluff Body Aerodynamics. En Y. Tamura, & A. Kareem (Edits.), Advanced Structural Wind Engineering (1 ed., pps. 59-84). Japan: Springer .
[10]. Crowe, C., Elger, D., & Roberson, J. (2002). Mecánica de los Fluidos (7th edition, 1st. edition in spanish). México D.F., México: C.E.C.S.A.

Anabel Apcarian Effect of Rotor Position on Wind Loads Acting on the Tower of a Stopped Wind Turbine." IOSR Journal of Mechanical and Civil Engineering (IOSR-JMCE) , vol. 14, no. 5, 2017, pp. 01-08.